Four-Port Nanophotonic Frustrated Total Internal Reflection Coupler

Duncan L. MacFarlane, Marc P. Christensen, Ke Liu, Tim P. LaFave, Jr., Gary A. Evans, Nahid Sultana,
T. W. Kim, Jiyoung Kim, Jay B. Kirk, Nathan Huntoon, Andrew J. Stark, Mieczyslaw Dabkowski,
Louis R. Hunt, and Viswanath Ramakrishna

Abstract—**Four-port frustrated total internal reflection couplers in InP-based GaInAsP quantum-well substrates are realized and characterized. Each coupler forms an "X" at the perpendicular intersection of two ridge waveguides and is aligned 45° to the optical path. The 180-nm-wide couplers are fabricated by dry etching deep trenches through the quantum wells and backfilling with alumina ($n = 1.71$) by atomic layer deposition. Coupling coefficients for the fabricated coupler are in good agreement with a three-dimensional finite-difference time-domain theory, and an 82% coupler efficiency is estimated.**

Index Terms—**Frustrated total internal reflection, integrated photonics, nanophotonics.**

I. INTRODUCTION

INDIUM phosphide (InP)-based photonic integrated circuits (PICs) represent a significant technological innovation that offers a multitude of advantages such as high functionality, improved efficiency, reduced space and power consumption, and lower costs [1]. A useful building block for many PICs is a photonic coupler capable of splitting an incoming signal into a number of different waveguides and combining multiple incoming signals into a single waveguide. Typical optical couplers are realized by a tapered Y-branch [2], parallel waveguides [3] or multimode interference [4]. These couplers are either limited by a long interaction length or large amounts of real estate. Photonic crystal based optical couplers are compact but hampered by inherently poor coupling efficiencies [5]. A recently reported compact, low loss silicon-on-insulator (SOI) rib waveguide with a 90° bend using a trench-based mirror [6] demonstrates the potential formation of a small footprint splitter/coupler.

In this letter, we discuss the theory, fabrication, and characterization of a four-port nanophotonic frustrated total internal reflection (FTIR) coupler realized in GaInAsP/InP.
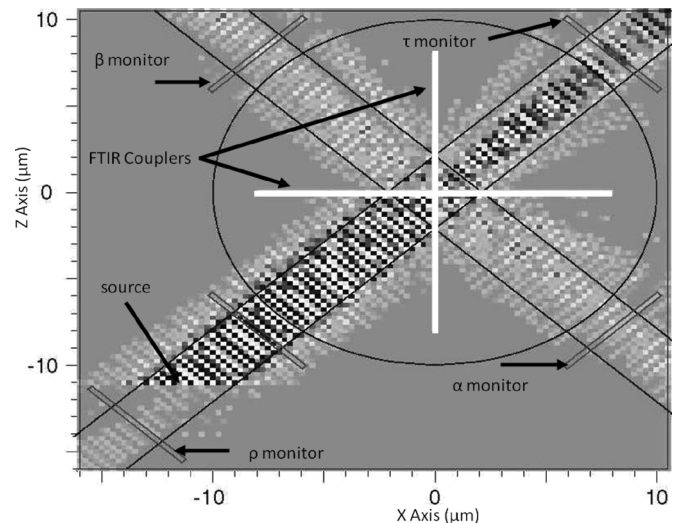
Fig. 1. FDTD analysis of a 180-nm-wide alumina-filled FTIR four-port nanophotonic coupler in InP/GaInAsP waveguides.

II. FTIR-BASED COUPLER THEORY

The four-port nanophotonic coupler presented is premised on the phenomenon of frustrated total internal reflection (FTIR) [7]. The couplers are formed by deep narrow trenches etched to completely overlap a waveguide mode. The trench is sufficiently narrow to support evanescent coupling (or tunneling) for transmission in addition to reflection. Arbitrary splitting ratios can be achieved in this configuration through careful selection of material properties and coupler width [8]. Examples of trench-based FTIR couplers have been previously demonstrated in both SOI [9] and InP-based quantum well substrates [10].

The coupler forms the shape of an "X" at the perpendicular intersection of two waveguides and is aligned 45° with respect to the optical path. Fig. 1 shows a three-dimensional finite difference time domain (FDTD) simulation of the four port nanophotonic coupler. This FDTD model is based on a three-layer approximation of the InP quantum well structure, but otherwise matches the fabricated device [11]. The simulation is performed using RSoft's FullWAVE Ver. 6.2, a commercial FDTD tool. The spatial grid size is 0.015 μm for the XYZ computational domain, respectively. The width 0.12 μm of perfectly matched layer is used as a boundary condition. The time step 0.005 is set to satisfy the Courant condition. As shown in Fig. 1, there are four coupler coefficients including reflection, ρ, transmission, τ, right-reflection, α, and left-reflection, β. The output power for each port is monitored and recorded, and the theoretical efficiency of the coupler is calculated by the power summation
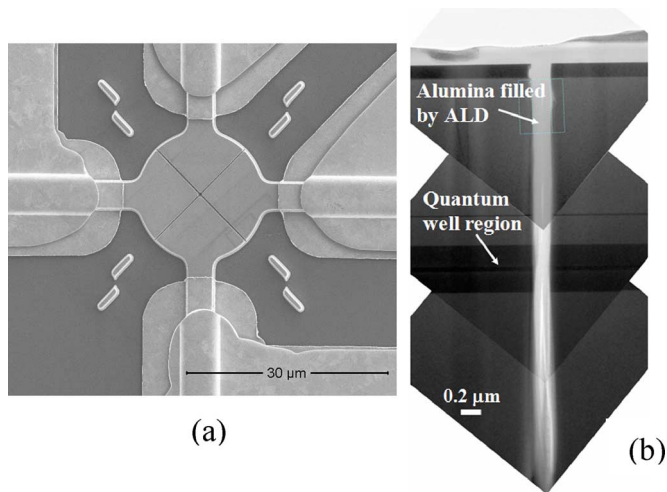
Fig. 2. (a) SEM of a four-port nanophotonic coupler with metal contacts. (b) Cross-sectional TEM image of the nanophotonic coupler.
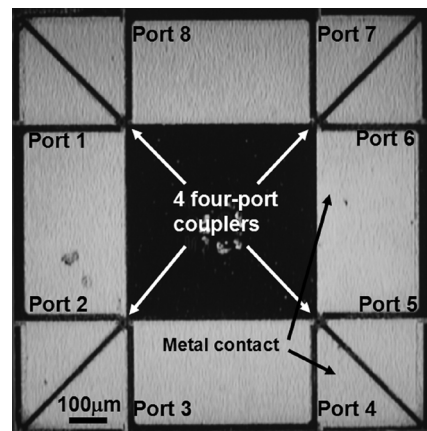

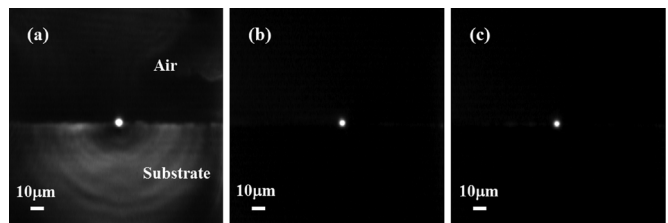Fig. 3. Optical micrograph of the two-dimensional active lattice filter.

Fig. 4. Near-field mode intensity profiles through the two-dimensional active lattice filter from an external light source. Light from (a) port 1 to port 6, (b) port 1 to port 5, and (c) port 2 to port 6.

of the four ports divided by the input power. An efficiency of $\sim 86\%$ is obtained by FDTD.

III. FABRICATION

The four-port nanophotonic FTIR coupler described herein is an enabling component of a two-dimensional active lattice filter [12], [13]. The coupler consists of a 20 μm $\times$ 180 nm $\times$ 3.9 μm trench etched through the epilayers of a typical waveguide structure grown on an InP substrate using HBr inductively coupled plasma (ICP) reactive ion etching (RIE) then filled with alumina (refractive index, $n \sim 1.71$) by atomic layer deposition (ALD). Following conventional ridge waveguide formation, the main process steps for the coupler fabrication consist of coupler patterning by focused ion beam (FIB), nanoscale trench etching by HBr-based ICP and alumina backfilling by ALD. Preparation for coupler trench etching [14] is conducted in several steps. A 1.0 μm SiO$_2$ film is deposited using a Unaxis 790 plasma-enhanced chemical vapor deposition system. A ~ 50 nm film of 2% polymethyl methacrylate (PMMA) is spun onto the sample. Once the PMMA film dries a ~ 70 nm thin film of chromium (Cr) is deposited using a Temescal e-beam evaporator. Nanopatterning of the Cr film is performed in an FEI Nova 200 focused ion beam (FIB) tool to define the metal hard mask used for reactive ion etching of the SiO$_2$ film. After FIB milling, the SiO$_2$ mask is dry etched to the depth of the InP by CHF$_3$/Ar using a Plasma-Therm ICP tool. The PMMA and Cr films are lifted-off to reveal the underlying SiO$_2$ pattern. High aspect ratio etching of trenches in InP is conducted using an HBr-based ICP chemistry at 165°C in an STS tool. Fig. 2(a) shows a four-port coupler visible in the scanning electron micrograph (SEM) as an "X." Trenches are then backfilled with alumina by ALD, a process chosen for its superior conformal deposition characteristics of high aspect ratio features. Alumina is deposited using a Cambridge NanoTech Savannah 200 ALD system. Fig. 2(b) shows a cross-sectional transmission electron micrograph (TEM) of a high-aspect ratio trench filled with a solid film of alumina. The trench width is ~ 180 nm. The overall trench depth, extending through the quantum well region to cover the optical, is ~ 3.9 μm.

IV. COUPLER CHARACTERIZATION

An optical micrograph of a two-dimensional active lattice filter consisting of 4 four-port nanophotonic couplers is shown in Fig. 3. In Fig. 4 is shown the near field intensity profile at an output of the two-dimensional active lattice filter measured with a standard end-fire coupling setup. The incident light at $\lambda = 1.55$ μm was coupled into the device via a tapered lens fiber. These images were recorded with an infrared camera. Transmission through the coupler was determined by coupling into port 1 and measuring the near-field mode from port 6. Reflection by the coupler was similarly determined by coupling into port 1/port 2 and measuring the near-field mode from port 5/port 6. Mode images are shown in Fig. 4(a)–(c), respectively.

To characterize the four-port couplers, incident light at $\lambda = 1.55$ μm with 190 μW power was coupled into each port of the eight-port coupler. The output powers at six other ports were measured in succession using an optical power-meter through a multimode fiber. The power of the output port on the same side as the input port cannot be measured due to setup limitations. There are a total of 48 pairs of power measurements at the input/output ports.

If the four-port couplers are assumed to have been identically fabricated, then there are five distinct light paths in the active lattice filter device, including port 1 to port 4, port 1 to port 5, port 1 to port 6, port 1 to port 7, and port 1 to port 8. Thus, the 48 pairs of power measurements may be reduced to 5 pairs by averaging measurements to obtain coefficients for an average coupler. However, in the device tested, the path of port 1 to port 6 was observed to yield more scattered light around the mode spot (cf. Fig. 4(a)) compared to other paths and may introduce

TABLE I
AVERAGED POWER FOR FOUR LIGHT PATHS IN THE TWO-DIMENSIONAL
ACTIVE LATTICE FILTER DEVICE

Input port (μW)	Output ports (μW)			
1	4	5	7	8
190	0.064	0.062	0.241	3.246

TABLE II
FOUR-PORT COUPLER POWER COEFFICIENTS AND EFFICIENCY
($\eta = \alpha + \beta + \tau + \rho$) CONSISTENT WITH MEASUREMENTS

	α	β	τ	ρ	η
P_{74}	0.16	0.12	0.23	0.32	0.83
P_{84}	0.13	0.12	0.22	0.32	0.79
P_{75}	0.19	0.14	0.25	0.28	0.86
P_{85}	0.15	0.18	0.23	0.29	0.85
P_{87}	0.15	0.14	0.17	0.30	0.76

larger than permissible error for an estimation of efficiency. The averaged measurement for this path is thus removed. The averaged power measured for four light paths is shown in Table I.

Transfer functions between each pair of input/output ports may be derived using a state space modeling approach [9], [10]. The modeling is used to evaluate four coupler coefficients, α, β, τ, and ρ. Considering port 1 as an input, the transfer function of a given output with respect to port 1 is a function of the coupler coefficients. For example, the transfer function from port 4 to port 1 may be written as, $H_{41} = f(\alpha, \beta, \tau, \rho)$. We set $z = 1$ since the measurement of power at the output ports is a steady state, continuous wave.

We set α, β, τ, and ρ in the scan range of 0 to 1.0 with resolution of 0.01. The four transfer functions, H_{41}, H_{51}, H_{71}, and H_{81} are numerically calculated. Let the ratio of power measured at the ith and jth output ports be $P_{ij} = H_{i1}/H_{j1}$. The data combination of four coupler coefficients is determined herein. Based on the FDTD analysis of a four-port coupler in Section II, the physical constraints $(\alpha + \beta + \tau + \rho) < 1.0$, $\rho > \tau$, $\rho > (\alpha, \beta)$, and $\tau > (\alpha, \beta)$, were used to guide convergence. The match tolerance between experiment and theory is controlled within 2% for each case. Computed coupler coefficients and efficiency are summarized in Table II. Further, the coupler coefficients and efficiency are averaged, and $\alpha = 0.156$, $\sigma_\alpha = 0.020$, $\beta = 0.140$, $\sigma_\beta = 0.022$, $\tau = 0.220$, $\sigma_\tau = 0.027$, $\rho = 0.302$, $\sigma_\rho = 0.016$, and $\eta = 0.818$, $\sigma_\eta = 0.038$, where σ is the root-mean-square value. An efficiency of $\sim 82\%$ is thus estimated for the novel four-port FTIR-based nanophotonic coupler, a value close to the theoretical limit of the coupler of these dimensions and composition.

V. CONCLUSION

We have designed, fabricated, and characterized four-port FTIR-based nanophotonic couplers in GaInAsP/InP ridge waveguides. A coupler efficiency of $\sim 82\%$ is estimated from optical power measurements made at each pair of input/output

ports. The interaction length of the coupler is on the order of the waveguide width, which represents a 100-fold footprint reduction on a chip. The minimal footprint of the compact nanophotonic coupler makes them a promising technology for dense planar photonic integrated circuits.

REFERENCES

[1] D. F. Welch, F. A. Kish, S. Melle, R. Nagarajan, M. Kato, C. H. Joyner, J. L. Pleumeekers, R. P. Schneider Jr., J. Bäck, A. G. Dentai, V. G. Dominic, P. W. Evans, M. Kauffman, D. J. H. Lambert, S. K. Hurtt, A. Mathur, M. L. Mitchell, M. Missey, S. Murthy, A. C. Nilsson, R. A. Salvatore, M. F. Van Leeuwen, J. Webjorn, M. Ziari, S. G. Grubb, D. Perkins, M. Reffle, and D. G. Mehuys, "Large-scale InP photonic integrated circuits: Enabling efficient scaling of optical transport networks," *IEEE J. Sel. Topics Quantum Electron.*, vol. 13, no. 1, pp. 22–31, Jan./Feb. 2007.

[2] H. Mizuno, O. Sugihara, T. Kaino, N. Okamoto, and M. Ohama, "Compact Y-branch-type polymeric optical waveguide devices with large-core connectable to plastic optical-fibers," *Jpn. J. Appl. Phys.*, vol. 44, no. 12, pp. 8504–8506, Dec. 2005.

[3] X. G. Tu, S. S. N. Ang, A. B. Chew, J. H. Teng, and T. Mei, "An ultracompact directional coupler based on GaAs cross-slot waveguide," *IEEE Photon. Technol. Lett.*, vol. 22, no. 17, pp. 1324–1326, Sep. 1, 2010.

[4] R. Halir, A. Ortega-Moñux, Í. Molina-Fernández, J. G. Wangüemert-Pérez, P. Cheben, D.-X. Xu, B. Lamontagne, and S. Janz, "Compact high-performance multimode interference couplers in silicon-on-insulator," *IEEE Photon. Technol. Lett.*, vol. 21, no. 21, pp. 1600–1602, Nov. 1, 2009.

[5] H.-T. Chien, C. Lee, H.-K. Chiu, K.-C. Hsu, C.-C. Chen, J. A. Ho, and C. Chou, "The comparison between the graded photonic crystal coupler and various couplers," *J. Lightw. Technol.*, vol. 27, no. 14, pp. 2570–2574, Jul. 15, 2009.

[6] Y. Qian, S. Kim, J. Song, and G. P. Nordin, "Compact and low loss silicon-on-insulator rib waveguide 90° bend," *Opt. Express*, vol. 14, no. 13, pp. 6020–6028, Jun. 2006.

[7] S. Zhu, A. W. Yu, D. Hawley, and R. Roy, "Frustrated total internal reflection: A demonstration and review," *Amer. J. Phys.*, vol. 54, no. 7, pp. 601–607, Jul. 1986.

[8] N. R. Huntoon, M. P. Christensen, D. L. MacFarlane, G. A. Evans, and C. S. Yeh, "Integrated photonic coupler based on frustrated total internal reflection," *Appl. Opt.*, vol. 47, no. 30, pp. 5682–5690, Oct. 2008.

[9] Y. Qian, J. Song, S. Kim, and G. P. Nordin, "Compact 90° trench-based splitter for silicon-on-insulator rib waveguides," *Opt. Express*, vol. 15, no. 25, pp. 16712–16718, Dec. 2007.

[10] U. Krishnamachari, S. Ristic, C.-H. Chen, L. Johansson, A. Ramaswamy, J. Klamkin, E. Norberg, J. E. Bowers, and L. A. Coldren, "InP/InGaAsP-based integrated 3-dB trench couplers for ultra-compact coherent receivers," *IEEE Photon. Technol. Lett.*, vol. 23, no. 5, pp. 311–313, Mar. 1, 2011.

[11] Y. Yuan, R. Jambunathan, J. Singh, and P. Bhattacharya, "Finite-difference time-domain analysis and experimental examination of the performance of a coupled-cavity MQW laser/active waveguide at 1.54 μm," *IEEE J. Quantum Electron.*, vol. 33, no. 3, pp. 408–415, Mar. 1997.

[12] A. E. El Nagdi, L. R. Hunt, D. L. MacFarlane, and V. Ramakrishna, "Extended active tunable optical lattice filters enabled by four-dimensional couplers: Systems modeling," *J. Opt. Soc. Amer. A*, vol. 26, no. 8, pp. A1–A10, Aug. 2009.

[13] A. E. El Nagdi, K. Liu, T. P. LaFave Jr., L. R. Hunt, V. Ramakrishna, M. Dabkowski, D. L. MacFarlane, and M. P. Christensen, "Active integrated filters for RF-photonic channelizers," *Sensors*, vol. 11, no. 2, pp. 1297–1320, Jan. 2011.

[14] N. Sultana, W. Zhou, T. P. LaFave Jr., and D. L. MacFarlane, "HBr based inductively coupled plasma etching of high aspect ratio nanoscale trenches in InP: Considerations for photonic applications," *J. Vac. Sci. Technol. B*, vol. 27, no. 6, pp. 2351–2356, Nov./Dec. 2009.